JACS
JOURNAL OF THE AMERICAN CHEMICAL SOCIETY
Communication
pubs.acs.org/JACS

Mechanism of H_2O Insertion and Chemical Bond Formation in $AlPO_4$-54·xH_2O at High Pressure

Frederico G. Alabarse,[†] Jérôme Rouquette,[†] Benoît Coasne,[†,‡] Abel Haidoux,[†] Carsten Paulmann,[§] Olivier Cambon,[†] and Julien Haines*[,†]

[†]Institut Charles Gerhardt Montpellier, UMR 5253 CNRS-Université de Montpellier-ENSCM, 34095 Montpellier Cedex 5, France
[‡]MultiScale Material Science for Energy and Environment (UMI CNRS/MIT), Massachusetts Institute of Technology, Cambridge, Massachusetts 02319, United States,
[§]Department Geowisssenschaften, Universität Hamburg, Hamburg, Germany

Supporting Information

ABSTRACT: The insertion of H_2O in $AlPO_4$-54·xH_2O at high pressure was investigated by single-crystal X-ray diffraction and Monte Carlo molecular simulation. H_2O molecules are concentrated, in particular, near the pore walls. Upon insertion, the additional water is highly disordered. Insertion of H_2O (superhydration) is found to impede pore collapse in the material, thereby strongly modifying its mechanical behavior. However, instead of stabilizing the structure with respect to amorphization, the results provide evidence for the early stages of chemical bond formation between H_2O molecules and tetrahedrally coordinated aluminum, which is at the origin of the amorphization/reaction process.

Water insertion in solids is of great importance in clays, concrete, zeolites, hybrid materials, such as metal organic frameworks, and carbon nanotubes as it modifies the material's properties and can lead to new technological applications.[1−6] In the case of water insertion in microporous materials, such as zeolites, superhydration effects are observed with a significant change in the mechanical properties of the material.[7−11] The mechanical response to water intrusion in the pores can lead to new possible applications of these materials as molecular springs and bumpers.[1,2,12−14] Water insertion also modifies the stability of porous materials with respect to amorphization.[11] Pressure-induced amorphization (PIA) is also commonly observed in such open framework structures and may confer useful properties in these materials for new potential applications, related to their high porosity, in the field of the absorption of mechanical shocks.[15]

$AlPO_4$-54·xH_2O is a hydrated aluminophosphate with the hexagonal VFI structure (space group $P6_3$)[16] with a = 18.9678(13) Å and c = 8.0997(4) Å, Z = 18.[17] This material exhibits 1-D pores along the **c** direction, which are among the largest pores known for zeolites and aluminophosphates with a diameter of 12.7 Å. The framework is built up of 4-, 6-, and 18-membered rings of alternating AlO_6, AlO_4, and PO_4 polyhedra. The octahedra contain two H_2O molecules, and additional H_2O molecules form a disordered hydrogen-bonded network in the pores. Based on X-ray powder diffraction and Raman spectroscopy,[11] H_2O insertion was found to decrease the onset of amorphization in this material from 2.0 to 0.9 GPa. Superhydration effects were observed, and an *increase* in the unit cell volume is observed at low pressures due to insertion of the H_2O molecules in the pores. Ex situ solid state NMR and X-ray absorption spectroscopy measurements[11] indicate that a certain amount of H_2O molecules enter the coordination sphere of the AlO_4 tetrahedra increasing the Al coordination number to 6.

Up to now, the mechanism of water insertion, chemical bond formation, and amorphization in this material is not yet understood. In the present study by synchrotron single-crystal X-ray diffraction and Monte Carlo molecular simulation, new insight into water intrusion and its chemical reaction with the aluminophosphate framework is obtained. These results are of relevance to other classes of porous or layered materials.[4−6]

Single crystals of $AlPO_4$-54·xH_2O were synthesized from alumina nanopowder (PURAL SB) and polyphosphoric acid by an optimized sol−gel procedure followed by hydrothermal treatment as described previously.[17] The needle-like single crystals (30 × 30 × 230 μm^3) were studied at high pressure in Merrill-Bassett diamond anvil cells with either beryllium or Boehler-Almax backing plates. The crystals were placed in 250 μm diameter, 120 μm thick tungsten gaskets along with a ruby sphere and either DAPHNE 7474[18] or H_2O as a pressure transmitting medium. DAPHNE 7474, which is based on alkyl silanes and silicone oil, does not enter the pores of $AlPO_4$-54·xH_2O and remains hydrostatic up to 3.7 GPa. Pressure was measured by the ruby fluorescence method.[19] X-ray diffraction experiments (λ = 0.500 Å) were performed on the 4-circle diffractometer on the F1 beamline at HASYLAB (DESY, Hamburg). Phi scans were performed with a MARCCD detector placed at 80.5 mm from the sample. Indexing and data reduction were performed using CrysalisPro (Agilent). The data were corrected for absorption using Absorb 7.0.[20] Average 2.22 was used to merge the data and reject outliers (http://www.rossangel.com/text_average.htm). Structure refinements were performed using SHELXL97.[21] F_{obs} Fourier maps were calculated using WinGX.[22] The crystal recovered after compression in H_2O was studied by X-ray diffraction on an Agilent Xcalibur diffractometer using Mo K_α radiation.

Received: November 4, 2014
Published: January 7, 2015

DOI: 10.1021/ja511153n
J. Am. Chem. Soc. 2015, 137, 584−587

Monte Carlo (MC) simulations were performed to probe water adsorption in $AlPO_4$-54·xH_2O. MC simulations in the Grand Canonical ensemble (constant chemical potential μ, volume V, and temperature T) were performed to determine the number of water molecules $n(P)$ per unit cell as a function of pressure P (obtained from μ and T using the ideal gas law). $n(P)$ = 47 in the closed system at 1.2 GPa and 49 in the open system at 0.5 GPa. These simulations allow comparison with our experiments, in which water is the pressure transmitting medium. Starting with water adsorbed at the bulk saturating vapor pressure, we also performed MC simulations in the Canonical ensemble (constant n, V, and T). Such simulations allow comparison with experiments with DAPHNE 7474 as the pressure transmitting medium. For each simulation, the sample unit cell was adjusted to reproduce that observed in the experiments in water and DAPHNE 7474 pressure transmitting media, respectively. Experiments on water in $AlPO_4$-54·xH_2O[17] showed that a few water molecules (labeled OW1 and OW2) have very low atomic displacements similar to that for the $AlPO_4$ atoms. This result, which suggests that these molecules are in such a strong interaction with the framework that they are nearly immobile, is in agreement with *ab initio* calculations in which a few water molecules were found to be linked to the framework.[23] The center of mass of OW1 and OW2 were thus frozen in the simulations. For each simulation, the AlPO4-54 structure was relaxed using a force field developed for these materials while imposing the experimental cell parameters. Small differences between the experimental and simulated structures (angles, compressibility, etc.), should have a very small effect on the structure and number of water molecules.

In the high-pressure X-ray diffraction studies, the maximum pressures were chosen as to avoid the onset of irreversible amorphization. A first experiment in H_2O was performed with measurements at 0.7 and 2.7 GPa. The crystal quality was already found to degrade at 0.7 GPa based on the high R-factors obtained. Beginning from the structural model at ambient pressure (space group $P6_3$),[17] the structure of $AlPO_4$-54·xH_2O was thus refined at 0.4, 0.7, and 1.2 GPa in DAPHNE 7474 and at 0.2 and 0.5 GPa in H_2O. In the latter experiment with a maximum pressure of 0.5 GPa, the changes observed at high pressure were found to be reversible as the recovered sample at ambient pressure was found to have equivalent cell parameters (a = 18.966(7) Å and c = 8.100(2)Å), and the fractional atomic coordinates were very similar to those of the starting material. As in the study at ambient pressure,[17] the occupancy of the disordered H_2O molecules in the pores was fixed to 50% giving 36 H_2O molecules per unit cell (x = 2). The further 11 H_2O molecules identified by MC simulations are too mobile to be localized by X-ray diffraction. The results at high pressure indicate that there is a concentration of H_2O molecules both near the pore walls and hydrogen-bonded to the H_2O molecules in the Al coordination sphere (Figure 1). Fourier difference maps confirmed this result obtained from the starting model. No significant difference was observed between the data obtained in DAPHNE 7474 and in H_2O indicating that the additional H_2O, which enters the pores when H_2O is used as a pressure transmitting medium giving rise to the superhydration effect, is liquid-like and x is greater than 2. This is in very good agreement with the results of MC simulations, which also indicate that there is a concentration of H_2O molecules near the pore walls and hydrogen bonded to the H_2O molecules of the AlO_6 octahedra. The simulated radial density at 0.5 GPa in H_2O shows the large density of water near the pore walls while

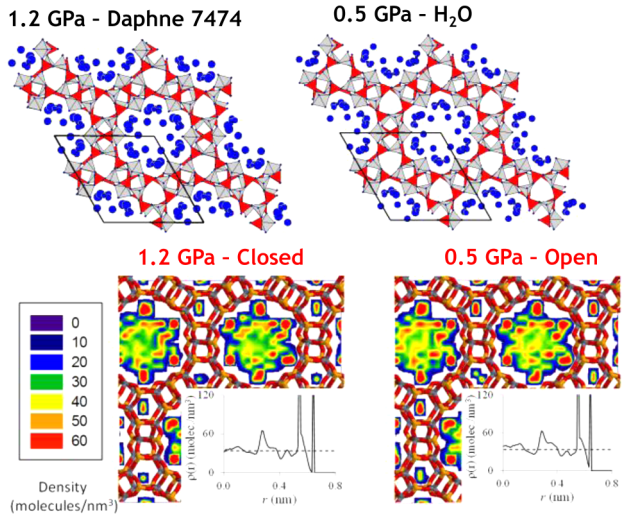

Figure 1. Structure and unit cell (outlined in black) of the $AlPO_4$-54·xH_2O framework (polyhedra) and oxygen atoms from the H_2O guest molecules (blue circles) at 1.2 and 0.5 GPa (top) and corresponding simulated density maps of water in $AlPO_4$-54·xH_2O in a closed and open system at the same pressures with the radial density of confined water given in the insets (bottom).

the broader distribution in the pore center suggests that water exhibits a disordered structure (Figure 1). Such a liquid-like structure was confirmed by determining the number n_{OH} of hydrogen bonds per water and tetrahedral order parameter q for confined water[17] (Supporting Information (SI)). Even if hydrogen bonds with the host matrix are considered, n_{OH} < 3.6 remains lower than the value for ice (n_{OH} = 4). Moreover, regardless of the position in the pore, q < 0.597 is lower than the value for ice (q = 1).

The present structural data allow the response of the $AlPO_4$-54·xH_2O structure and pore network to water insertion to be understood. Water insertion strongly modifies the compressibility of $AlPO_4$-54·xH_2O. In contrast to the results obtained using the nonpenetrating pressure transmitting medium DAPHNE 7474, in H_2O, the compressibility along **c** is much lower and **a** is initially incompressible due to water insertion (Figure 2). The pore height (i.e., c cell parameter) is more compressible than the pore diameter (i.e., O−O distance across the pore reduced by 2 × oxygen radius of 1.35 Å) in both fluids. In H_2O, the compressibility of the pore is similar to that of the a cell parameter, whereas in DAPHNE 7474 the pore diameter decreases to a greater extent than a. This indicates that the compressibility of the pores is very similar to that of the framework due to water intrusion using H_2O as a pressure transmitting medium with a decrease in both pore and unit cell volumes of close to 1% from 0.1 MPa to 0.5 GPa; thus the porosity remains constant. In contrast, the pore diameter decreases more rapidly than a in DAPHNE 7474, and consequently the porosity decreases in a continuous way from 40.7% at ambient pressure to 40.3% at 1.2 GPa. The corresponding decrease in unit cell and pore volumes are 4.9% and 5.8%, respectively.

The response of the framework can be principally linked to changes in the interpolyhedral Al−O−P bridging angles, as the polyhedra are essentially rigid up to the maximum pressure reached of 1.2 GPa (see SI). A major effect of H_2O insertion on the structure is to significantly lower the pressure dependence of the various angles (Figure 3). The corresponding angles in

DOI: 10.1021/ja511153n
J. Am. Chem. Soc. 2015, 137, 584−587

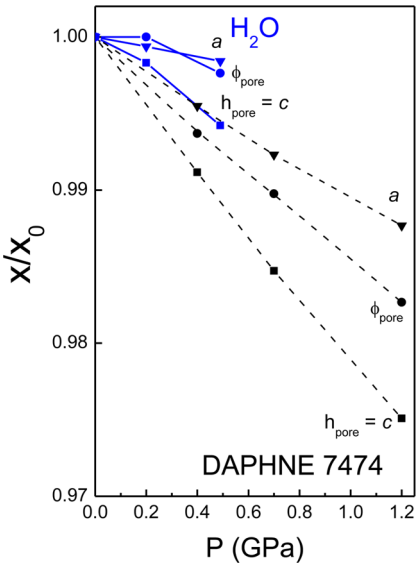

Figure 2. Relative compression of the unit cell parameters *a* and *c* and the pore diameter ϕ and height *h* in water (blue) and Daphne 7474 (black).

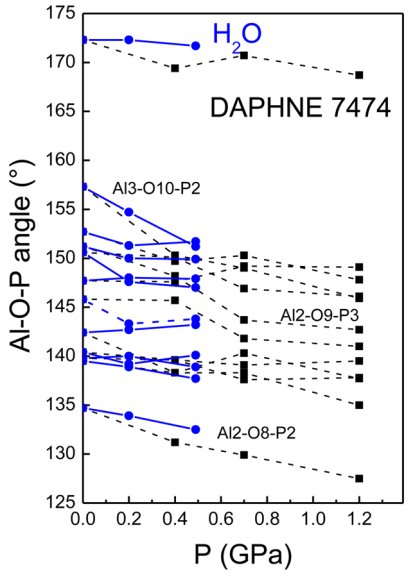

Figure 3. Relative compression of the Al−O−P bridging angles in water (blue) and Daphne 7474 (black).

the experiment in DAPHNE 7474 decrease to a much greater extent. The out-of-plane bridging angles exhibit the strongest decreases of 7°−11° between ambient and 1.2 GPa (Figure 3 and SI), whereas the in-plane angles are more stable. The out-of-plane bridging angles correspond to intertetrahedral bridging angles, which directly influence the *c* cell parameter. The ring systems in the *xy* plane, double 4-membered rings (4MR), six-membered rings (6MR), which form the 18-membered ring corresponding to the pores, are particularly rigid.

F_{obs} Fourier maps were calculated in order to have additional information on the location of the H_2O molecules in the structure (Figure 4). The regions of highest density correspond to the Al and P atoms, which form the 4MRs and 6MRs, with discrete regions of lower density corresponding to the localization of oxygen atoms. At ambient pressure, the occupation of H_2O molecules exhibits higher density near the

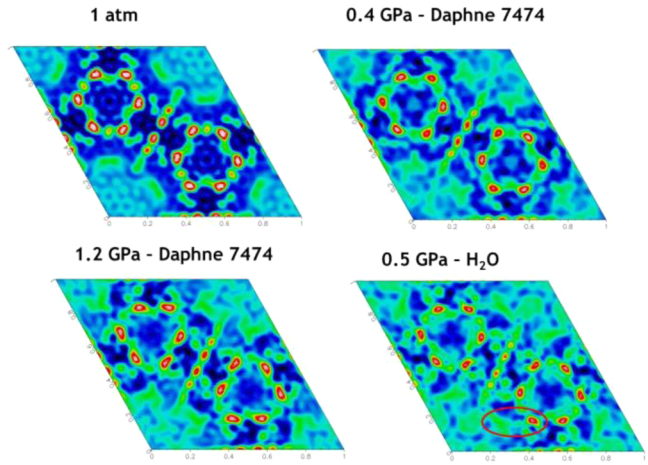

Figure 4. Observed Fourier maps F_{obs} of hydrated $AlPO_4$-54·$x$$H_2O$ at various pressures. Electron density increases according to the following color scale: blue (low), green, yellow, red, white (high). The red ellipse is a guide to the eye and highlights one of the regions of increased electron density corresponding to the migration of the oxygen atoms of H_2O toward the Al atoms.

pore walls at a distance of 2.8 Å governed by the formation of hydrogen bonds with the oxygen atoms of the framework. Upon increasing pressure in DAPHNE7474, a structuring of the pore water begins to occur, in which linking to the H_2O molecules in the AlO_6 octahedra and gradually migration toward the tetrahedral Al atoms in the 6MRs are observed. In H_2O, this behavior is much more pronounced with evidence for the beginning of the incorporation of some H_2O in the coordination sphere of tetrahedral Al at a distance of close to 2 Å. This is exactly what has been observed ex situ after decompression by solid state NMR. In this case, the initial stages of Al−O bond formation are directly observed in situ. This provides direct evidence for the mechanism of amorphization in this material linked to the change in coordination number of Al from 4 to 6, which is directly related to the amount of water molecules available in the pore. These results clearly show that this process begins at significantly lower pressure due to water insertion. Additionally, an increase in H_2O concentration at the pore center is observed at 0.5 GPa. This result is in good agreement with the MC simulations (Figure 1), which confirm the presence of water at the pore center and indicate the presence of two additional H_2O molecules per unit cell.

In conclusion, structure refinements for $AlPO_4$-54·$x$$H_2O$ were successfully performed using high-pressure, synchrotron, single crystal X-ray diffraction data. The analysis of the effect of pressure and H_2O insertion on the pore size and the localization of the H_2O molecules in the pores provides a detailed understanding of the insertion (superhydration and the presence of liquid-like H_2O at the pore center) and compression mechanisms (higher Al−O−P angles) in this material. The results also provide evidence for the early stages of bond formation between selected H_2O molecules and tetrahedral Al from the framework leading to amorphization of this material. These results are found to be in very good agreement with the density maps obtained from Monte Carlo simulations. In the present case, the incorporation of guest species favors amorphization due to the chemical reaction between the inserted water and the framework. This contrasts with previous studies[24−27] in which the incorporation of guest

DOI: 10.1021/ja511153n
J. Am. Chem. Soc. 2015, 137, 584−587

atoms or molecules stabilizes porous materials with respect to amorphization arising from the collapse of the pores. The difference in behavior is governed by the reactivity of the guest species with respect to the framework.

■ ASSOCIATED CONTENT

Supporting Information

Supporting Information contains additional data and a description of the computational methods and simulation parameters. This material is available free of charge via the Internet at http://pubs.acs.org.

■ AUTHOR INFORMATION

Corresponding Author

*Julien.Haines@univ-montp2.fr

Notes

The authors declare no competing financial interest.

■ ACKNOWLEDGMENTS

We would like to thank Manuel Hinterstein for assistance with the experiment at DESY, Ross Angel for useful discussions concerning absorption corrections, Keizo Murata and Stefan Klotz for providing the DAPHNE 7474 oil, Olaf Torno (SASOL) for supplying the PURAL SP, and Dominique Granier for technical assistance. We acknowledge the French National Research Agency (ANR) for funding through the research project ANR-09-BLAN-0018-01.

■ REFERENCES

(1) Eroshenko, V.; Regis, R. C.; Soulard, M.; Patarin, J. *J. Am. Chem. Soc.* **2001**, *123*, 8129.
(2) Karbowiak, T.; Paulin, C.; Ballandras, A.; Weber, G.; Bellat, J. P. *J. Am. Chem. Soc.* **2009**, *131*, 9898.
(3) Cailliez, F.; Trzpit, M.; Soulard, M.; Demachy, I.; Boutin, A.; Patarin, J.; Fuchs, A. H. *Phys. Chem. Chem. Phys.* **2008**, *10*, 4817.
(4) Coussy, O. *Mechanics and Physics of Porous Solids*; Wiley: New York, 2010.
(5) Guillou, N.; Millange, F.; Walton, R. I. *Chem. Commun.* **2011**, *47*, 713.
(6) You, S. J.; Kunz, D.; Stoeter, M.; Kalo, H.; Putz, B.; Breu, J.; Talyzin, A. V. *Angew. Chem., Int. Ed.* **2013**, *52*, 3891.
(7) Hazen, R. M. *Science* **1983**, *219*, 1065.
(8) Lee, Y.; Hriljac, J. A.; Vogt, T.; Parise, J. B.; Artioli, G. *J. Am. Chem. Soc.* **2001**, *123*, 12732.
(9) Lee, Y.; Vogt, T.; Hriljac, J. A.; Parise, J. B.; Artioli, G. *J. Am. Chem. Soc.* **2002**, *124*, 5466.
(10) Quartieri, S.; Montagna, G.; Arletti, R.; Vezzalini, G. *J. Solid State Chem.* **2011**, *184*, 1505.
(11) Alabarse, F. G.; Silly, G.; Haidoux, A.; Levelut, C.; Bourgogne, D.; Flank, A. M.; Lagarde, P.; Pereira, A. S.; Bantignies, J. L.; Cambon, O.; Haines, J. *J. Phys. Chem. C* **2014**, *118*, 3651.
(12) Bushuev, Y. G.; Sastre, G.; de Julian-Ortiz, J. V.; Galvez, J. *J. Phys. Chem. C* **2012**, *116*, 24916.
(13) Tzanis, L.; Trzpit, M.; Soulard, M.; Patarin, J. *J. Phys. Chem. C* **2012**, *116*, 20389.
(14) Guillemot, L.; Biben, T.; Galarneau, A.; Vigier, G.; Charlaix, E. *P. Natl. Acad. Sci. USA* **2012**, *109*, 19557.
(15) Haines, J.; Levelut, C.; Isambert, A.; Hebert, P.; Kohara, S.; Keen, D. A.; Hammouda, T.; Andrault, D. *J. Am. Chem. Soc.* **2009**, *131*, 12333.
(16) McKusker, L. B.; Baerlocher, C.; Jahn, E.; Bulow, M. *Zeolites* **1991**, *11*, 308.
(17) Alabarse, F. G.; Haines, J.; Cambon, O.; Levelut, C.; Bourgogne, D.; Haidoux, A.; Granier, D.; Coasne, B. *Phys. Rev. Lett.* **2012**, *109*, 035701.
(18) Murata, K.; Yokogawa, K.; Yoshino, H.; Klotz, S.; Munsch, P.; Irizawa, A.; Nishiyama, M.; Iizuka, K.; Nanba, T.; Okada, T.; Shiraga, Y.; Aoyama, S. *Rev. Sci. Instrum.* **2008**, *79*, 085101.
(19) Mao, H. K.; Xu, J.; Bell, P. M. *J. Geophys. Res.-Solid* **1986**, *91*, 4673.
(20) Angel, R.; Gonzalez-Platas, J. *J. Appl. Crystallogr.* **2013**, *46*, 252.
(21) Sheldrick, G. M. *Acta Crystallogr. A* **2008**, *64*, 112.
(22) Farrugia, L. J. *J. Appl. Crystallogr.* **2012**, *45*, 849.
(23) Poulet, G.; Tuel, A.; Sautet, P. *J. Phys. Chem. B* **2005**, *109*, 22939.
(24) Haines, J.; Cambon, O.; Levelut, C.; Santoro, M.; Gorelli, F.; Garbarino, G. *J. Am. Chem. Soc.* **2010**, *132*, 8860.
(25) Wei, Q.; Xu, H. W.; Yu, X. H.; Shimada, T.; Rearick, M. S.; Hickmott, D. D.; Zhao, Y. S.; Luo, S. N. *J. Appl. Phys.* **2011**, *110*, 056102.
(26) Fu, Y. Q.; Song, Y.; Huang, Y. I. *J. Phys. Chem. C* **2012**, *116*, 2080.
(27) Niwa, K.; Tanaka, T.; Hasegawa, M.; Okada, T.; Yagi, T.; Kikegawa, T. *Micropor. Mesopor. Mater.* **2013**, *182*, 191.

DOI: 10.1021/ja511153n
J. Am. Chem. Soc. 2015, 137, 584−587